PHYSICAL REVIEW E **90**, 030301(R) (2014)

Insertion and confinement of hydrophobic metallic powder in water: The bubble-marble effect

Yehuda Meir and Eli Jerby*
Faculty of Engineering, Tel Aviv University, Ramat Aviv, 69978 Tel Aviv, Israel
(Received 14 May 2014; published 11 September 2014)

Metallic powders such as thermite are known as efficient fuels also applicable in oxygen-free environments. However, due to their hydrophobicity, they hardly penetrate into water. This paper presents an effect that enables the insertion and confinement of hydrophobic metallic powders in water, based on encapsulating an air bubble surrounded by a hydrophobic metallic shell. This effect, regarded as an inverse of the known liquid-marble effect, is named here "bubble marble" (BM). The sole BM is demonstrated experimentally as a stable, maneuverable, and controllable soft-solid-like structure, in a slightly deformed hollow spherical shape of ∼1-cm diameter. In addition to experimental and theoretical BM aspects, this paper also demonstrates its potential for underwater applications, such as transportation of solid objects within BM and underwater combustion of thermite BM by localized microwaves. Hence, the BM phenomena may open new possibilities for heat and thrust generation, as well as material processing and mass transfer underwater.

DOI: 10.1103/PhysRevE.90.030301 PACS number(s): 82.70.Dd, 47.55.D−, 82.30.Nr, 82.30.Rs

Metallic powders such as thermite mixtures are known as efficient combustible fuels [1]. The thermite reaction also provides a mechanism for the production of ceramic materials (e.g., the conversion of rusty iron and aluminum to alumina [2]). Unlike carbon-based fuels, the thermite combustion does not need an external supply of oxygen (since it is provided by the oxide component within the mixture, e.g., $3Fe_3O_4 + 8Al \rightarrow 9Fe + 4Al_2O_3 + 3.67kJ/g$). Therefore, as zero-oxygen-balance fuel, thermite could have a great importance for underwater applications, such as heat and thrust generation, as well as for underwater transportation and construction operations [3]. The challenge, however, stems from the hydrophobic properties of these powders that impede their confinement and insertion directly into water [4].

Here we present an effect of a sole air bubble formation within a shell of hydrophobic powder in water, induced by a magnetic-field gradient. The resulting ∼1-cm-diameter powder-based structure is controllable and maneuverable in water. The new structure consists of an air core with a powder shell surrounded by water, whereas in the known liquid-marble (LM) the powder-encapsulated core is usually liquid and the surrounding substance is air. Hence, the new structure can be regarded to some extent as an *inverse* of the known LM effect, and is therefore coined here as a *bubble marble* (BM).

The known LM exhibits solid-like properties such as structural stability due to the binding force between the powder particles in its outer layer [5]. The LM's stable spherical structure is maintained by the attracting capillary forces among the powder particles in the coating layer, and by the consequent surface tension [6]. LM phenomena have found interests in various fields [7,8], including transport mechanisms, chemical reactions, and sensing. Magnetic and electric fields are also used to manipulate and control LM coated by magnetic powders, such as oil-based marbles coated by magnetite nanoparticles underwater [9,10]. Similar to droplets, foams also can be stabilized by hydrophobic particles [11]. Foams of micrometer-sized air bubbles provide enhanced contrast for ultrasound imaging. With magnetic shells, they can also be used as a contrast agent for magnetic resonance imaging (MRI) [12]. However, while single self-assembled LM with liquid core have been extensively observed and studied [5–8], the inverse effect of a sole controllable bubble comprising an air core and a powder shell in water has not yet been demonstrated.

The BM is initiated in the experiments presented here by a layer of hydrophobic powder floating on water, to which a magnetic-field gradient is externally applied. The powder is made as a mixture of microscale powders of magnetite (Fe_3O_4) and aluminum (Al). In the following experiments, Iron Black 318 and Aluminum-400 powders, with particle sizes $<45\ \mu$m and $<37\ \mu$m in a ratio of 3.2 : 1 by weight, respectively, are employed. The perpendicular magnetic field is generated by an electromagnet in the range 0–150 G, and is measured by a Hall probe (MG-5DP Walker Scientific Inc.). A high-speed video camera (SV-643C, 200 frames per second) is used to capture the BM dynamics. The BM volume is measured by the water level using Archimedes' law. BM inflation and deflation tests are performed here by injecting air into the BM as into an elastic balloon, using a 1.2-mm-diameter needle.

The powder initially floats and laterally agglomerates upon the liquid-air interface (due to the capillary forces induced between the particles). By applying a vertical inhomogeneous magnetic field, the magnetite is self-assembled to microstructures along the magnetic field (due to the inner dipole-dipole interaction [13]). By increasing the magnetic-field gradient, the powder layer concaves into the water (similarly to the Moses effect [14,15] but in a $\sim 10^2$ smaller magnetic field). Consequently, the floating powder layer undergoes a compactification and folds inside to form a hollow semispheroid. The latter further sinks into the water and finally forms a BM, as shown in Figs. 1(a)–1(d). The BM is sustained in water and can be manipulated and maneuvered by various magnetic and mechanical means as described below (and in the Supplemental Material [16]).

The initial sinking effect, shown in Fig. 1(b), is analyzed by varying the mass of the thermite batch poured on the water's surface, in the range $0.02 - 0.80$ g. Initially, before applying the magnetic field, the powder mixture floats and aggregates

*jerby@eng.tau.ac.il

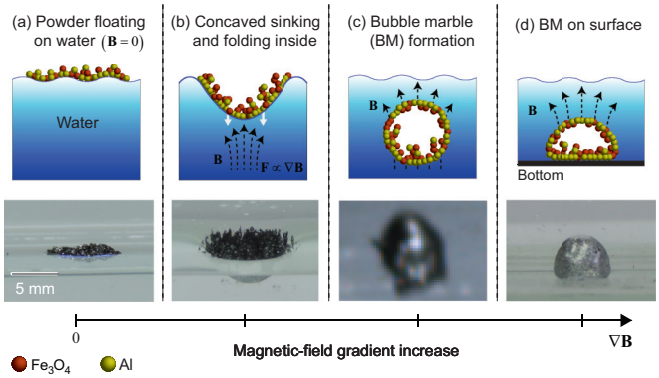

FIG. 1. (Color online) The initiation of a BM coated by thermite powder in water. The magnetic-field gradient pulls down the floating thermite layer (a), which then concaves in a Moses-like effect into the water (b). By a further increase of the magnetic-field gradient, the layer is folded inside to form a bubble marble (c), which then sinks to the bottom (d), toward the higher magnetic-field gradient near the magnetic pole.

on the water surface, despite the relatively large densities of bulk magnetite and aluminum (5.7 and 2.7 times larger than water, respectively). This floating is attributed to the lateral capillary forces between the hydrophobic aluminum-powder particles attached to the magnetite. Once the magnetic-field gradient is applied, the powder layer concaves as a membrane into a depth h in the water. Measurements of h with respect to the vertical magnetic-field gradient (represented by its average and difference values, $B_{\rm av}$ and ΔB, respectively, along h) are shown in Fig. 2.

Considerations of energy conservation [14] lead to the estimate

$$h = \frac{\chi}{\rho g \mu_0} B_{\rm av} \Delta B, \qquad (1)$$

where χ/ρ is the effective mass permeability of the floating medium, g is the gravitational acceleration, and μ_0

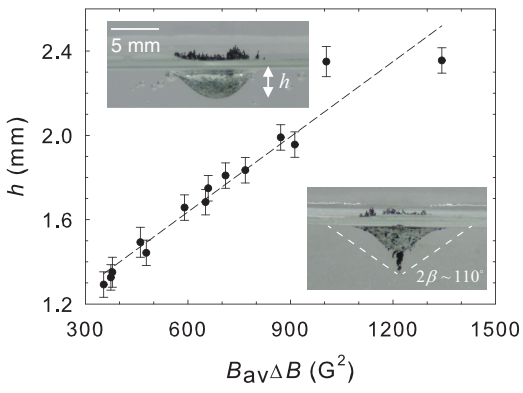

FIG. 2. (Color online) The sinking effect of the floating thermite surface layer, induced by the magnetic field. The graph shows the concave depth h with respect to the magnetic-field gradient. The Moses-like effect, shown in the insets, occurs here in a 10^2 smaller magnetic field than elsewhere [15]. The right-lower inset shows the conical shape obtained in a $2\beta \sim 110^\circ$ critical angle prior to the BM formation.

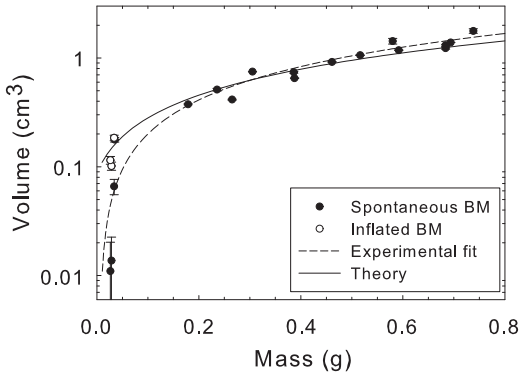

FIG. 3. The BM volume with respect to its mass. The solid and dashed lines show the theoretical predictions by Eq. (2) and the best fit of the experimental results, respectively. The graph shows the spontaneously generated BM volume, as well as three examples of small BM's inflated to their maximal volumes.

is the vacuum magnetic permeability [note that the term $B_{\rm av}\Delta B/\mu_0 \simeq (B_1^2 - B_2^2)/2\mu_0$ represents the magnetic-energy difference between the upper and lower magnetic fields (B_1 and B_2, respectively) where $B_{\rm av} = (B_1 + B_2)/2$]. A linear fit of the experimental results shows a slope of 1.2×10^{-3} mm/G^2. This ratio is $\sim 10^5$ larger here than in known Moses effect experiments [15] due to the mass susceptibility of the magnetite [$(\chi/\rho)_M = 4.8$ m^3/kg in a coarse powder [17] and $\sim 1.5 \times 10^{-3}$ m^3/kg effectively here]. The maximal crater depth is also evidenced by the final conical shape obtained (just before the BM formation) as shown in Fig. 2. Its critical angle is observed as $2\beta \sim 110^\circ$, in agreement with an analysis of self-assembled structures of magnetic powder under magnetic fields [18].

Once the BM has been created and has sunk to the bottom of the water tank, it is held there by the magnetic-field and hence deforms to a hemisphere shape, as shown in Fig. 1(d). The magnetic-field gradient can then be reduced below equilibrium, thus enabling the BM to rise up in a spherical-like shape. The threshold of the magnetic-field gradient is found as 7.5 ± 1.5 G/cm with a slight dependence on the mass. Experimental results of the BM volume obtained with respect to its mass are presented in Fig. 3.

A simplified model is derived to estimate the BM volume needed to be sustained underwater. The buoyancy force and the opposed vertical component of the magnetic force induced are given by $F_B = (\rho_w V - M)g$ and $F_M = SM\sigma_m(\nabla \mathbf{B})_\perp$, respectively, where V and M are the bubble volume and mass, respectively, $\mathbf{B}$ is the magnetic field vector, $S = 0.77$ is the magnetite to thermite stoichiometric mass ratio, and $\sigma_m = 82.4$ Am^2/kg is the magnetite's magnetic moment per mass [17]. An additional pulling force, $F_s = 2\gamma_{\rm Al} A/d$, is contributed by the BM surface area change when starting to rise up, where d and A are the BM diameter and area change, respectively ($2A/d \sim 1.6V^{1/3}$), and $\gamma_{\rm Al} = 0.12$ N/m is the aluminum powder surface tension [19]. The volume V of the BM related to its mass M in equilibrium state, $F_M + F_s = F_B$, shall therefore satisfy

$$\rho_w g V - 1.6\gamma_{\rm Al} V^{1/3} - SM\sigma_m(\nabla \mathbf{B})_\perp - Mg = 0. \qquad (2)$$

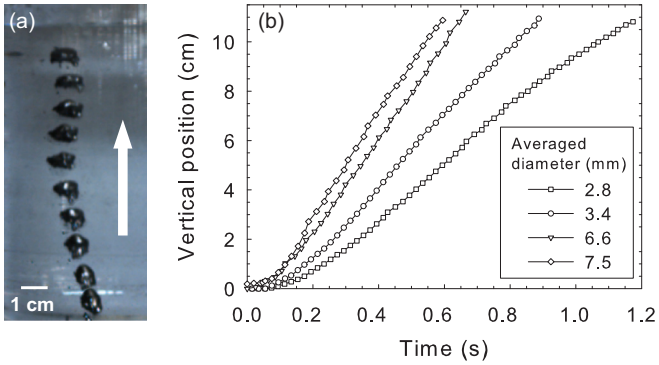

FIG. 4. (Color online) The BM floating up in water after the magnetic field is turned off: (a) Images of the BM rising up taken in 50-ms time intervals. (b) The vertical position vs. time of BM of various sizes, rising up spontaneously.

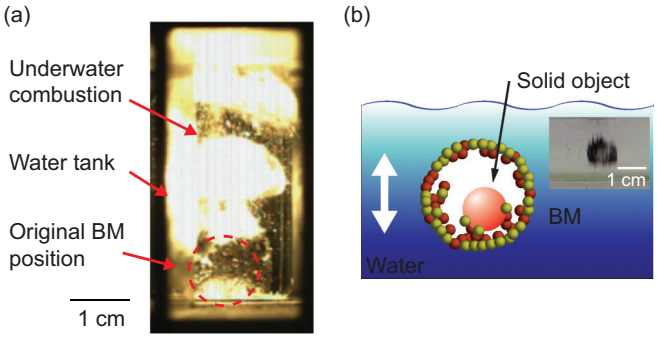

FIG. 5. (Color online) Examples for potential operations enabled by BM underwater, as demonstrated experimentally: (a) Ignition of pure-thermite BM using localized microwaves [25]. (b) Underwater transportation of objects captured inside BM. The inset shows an example of a chunk of glass lifted up by BM in a water tank, a ~4-cm height from its bottom to the surface (see Supplemental Material [16]).

The theoretical estimate of the BM volume versus mass presented in Fig. 3 coincides with the experimental results.

Once the magnetic field is turned off, the BM rises upwards from the bottom, retaining its shape until it reaches the water surface. Figures 4(a) and 4(b) show stroboscopic images of the BM rising up and its vertical position versus time for various sizes, respectively. The initial BM's acceleration a with respect to its diameter d is obtained by a second-order polynomial fit of the curves shown in Fig. 4(b) and results in a nearly linear relation $a \sim 2.9 \times 10^2 d - 0.45$. The rising speed of the BM is found here as $v \sim 0.8\sqrt{gd}$ in its steady state, close to the Haberman-Morton terminal velocity of a pure air bubble ($v_T = 0.7\sqrt{gd}$) [20]. The Reynolds number $\mathrm{Re} = \rho v d/\eta$ for a stable BM (where η is the water viscosity) results here in ~750, which is significantly high. The observations here show that the BM remains stable in this scale, while pure air bubbles with $\mathrm{Re} > 50$ are pierced by the jet stream and changed to a toroidal shape [21]. The BM remains stable below the critical length of 4κ (where $\kappa = 3.5$ mm is the water capillary length, $\kappa = \sqrt{\gamma_{\mathrm{Al}}/\rho_w g}$) [22]. Its Bond number is found to be in the range $0.3 - 7$ according to $\mathrm{Bo} = (d/\kappa)^2$, hence its shape is expected to be a spherical cap in rest and an oblate ellipsoid in motion [20], as experimentally observed here. When the BM rises up and reaches the water surface with no magnetic field, it is dispersed there and inversely decomposed to its original state of a floating powder layer [as in Fig. 1(a)]. However, when the tank is filled to the top with water, the BM's nearly spheroidal shape is preserved when reaching the tank's ceiling [similarly to Fig. 1(d) upside down].

The BM can be manipulated in various ways. It can be split mechanically, for instance, into two distinct BM's. A merging effect is observed as well, allowing two adjacent BM's to merge together and form a larger BM, which minimizes their surface energy. Once formed, the BM can be further inflated by injecting air into it, which increases its volume to a certain limit. Above this critical volume, the excess air is released by a secondary air bubble while the BM shape is preserved. Similarly, the BM can also be deflated and shrunk. The BM can also be frozen so that its shape is preserved in ice (e.g., for *ex situ* analyses). It is also noted that the magnetite spikes do not penetrate the BM outer shell, possibly due to the combination of the capillary force between the aluminum particles and the attractive force between the parallel magnetic dipoles [18]. Consequently, the aluminum particles are mostly seen on the outer BM layer, whereas the magnetite is observed inside the shell (in an analogy to the Janus armor effect [23], one face here is the outer hydrophobic sphere and the opposite one is the inner magnetic layer). Similar experiments in ethanol ($\rho_e = 0.79$ g/cm^3, $\gamma_e = 0.04$ N/m) [19] instead of water show that BM are not created in ethanol. The thermite powder does not form a floating surface layer, but entirely sinks instead even without a magnetic field (note that magnetite powder alone also sinks in water, but the thermite mixture does not due to the synergy of the two powder types).

The confinement of BM thermite underwater enables new possibilities, such as the effective ignition of thermite fuels underwater by localized microwaves (note that pure thermites are usually hard to ignite even in air atmosphere [24], and as yet there is no way available to initiate underwater combustion of such hydrophobic powders, unless by their previous coating or solidification to pellets [3,4]). It was found here that 2.45-GHz microwaves applied underwater to a pure-thermite BM ignite it almost instantaneously, causing a mushroom-like flame in the water, as shown in Fig. 5(a) [25]. The intense combustion heat energy (3.67 kJ/g) produced in this exothermic zero-oxygen balance reaction is transferred to the surrounding water, which also generates thrust due to its latent heat. The ignition effect is further enhanced by providing the microwave energy locally near the BM (e.g., by an open-end applicator as in air [24]). These findings may lead to novel means for underwater heat and thrust generation (e.g., for underwater construction works, novel marine engines, etc.).

The BM can also be used as a vehicle to trap an object and transport it in water, as illustrated in Fig. 5(b). This effect is demonstrated experimentally here for both light and heavy objects (relative to water). For instance, a paraffin chunk floating on water is captured by BM and carried inside it into the water, down to the bottom. Likewise, a heavy object made of glass, lying on the bottom of the water tank, is trapped by BM and lifted up to the water's surface (see Supplemental Material video clips [16]). Both cases demonstrate the BM's potential as an underwater carrier of objects.

In conclusion, the BM effect introduced here enables the creation and manipulation of a solely confined structure of hydrophobic metallic powder such as a thermite mixture, by forming a shell around an air bubble in water. The BM is considered here as an inverse of the known LM effect since it preserves some of the LM features in the different medium of underwater environment. Hence, the BM enables the insertion of hydrophobic powders into water, either solely in a hollow BM structure or as a vehicle for other objects carried in it. The BM also provides a means for underwater combustion of thermite fuels.

The findings presented here may stimulate fundamental studies of new BM phenomena, as well as practical developments of various BM applications. Future studies may aim for instance at finding other types of external force in order to form and manipulate BM of nonmagnetic powders (e.g., electrostatic forces [26]). The BM shining effect (seen in Figs. 1 and 4) might be hypothesized [27] as caused by a thin air layer trapped around the hydrophobic aluminum shell (as in Ref. [28]). Other studies may explore BM for combustion and thrust generation (e.g., for new types of marine engines), material processing and construction, and transportation underwater.

This study is supported by the Israel Science Foundation (ISF), Grant No. 1639/11.

[1] M. L. Pantoya and J. J. Granier, Propellants Explos. Pyrotech **30**, 53 (2005).
[2] Q. S. Meng, S. P. Chen, J. F. Zhao, H. Zhang, H. X. Zhang, and Z. A. Munir, Mater. Sci. Eng. A **456**, 332 (2007).
[3] S. C. Stacy, M. L. Pantoya, D. J. Prentice, E. D. Steffler, and M. A. Daniels, Adv. Mater. Process. **167**, 33 (2009).
[4] E. Nixon, M. L. Pantoya, G. Sivakumar, A. Vijayasai, and T. Dallas, Surf. Coat. Technol **205**, 5103 (2011).
[5] P. Aussillous and D. Quéré, Nature **411**, 924 (2001).
[6] E. Bormashenko, R. Pogreb, G. Whyman, and A. Musin, Colloids Surf. A, Physicochem. Eng. Aspects **351**, 78 (2009).
[7] G. McHale and M. I. Newton, Soft Matter **7**, 5473 (2011).
[8] E. Bormashenko, R. Balter, and D. Aurbach, Int. J. Chem. React. Eng. **9**, S10 (2011).
[9] Y. Zhao, J. Fang, H. Wang, X. Wang, and T. Lin, Adv. Mater. **22**, 707 (2010).
[10] L. Zhang, J. Wu, Y. Wang, Y. Long, N. Zhao, and J. Xu, J. Am. Chem. Soc. **134**, 9879 (2012).
[11] T. N. Hunter, R. J. Pugh, G. V. Franks, and G. J. Jameson, Adv. Colloid Interface Sci. **137**, 57 (2008).
[12] F. Yang, Y. Li, Z. Chen, Y. Zhang, J. Wu, and N. Gu, Biomaterials **30**, 3882 (2009).
[13] G. Pál, F. Kun, I. Varga, D. Sohler, and G. Sun, Phys. Rev. E **83**, 061504 (2011).
[14] N. Hirota, T. Homma, H. Sugawara, K. Kitazawa, M. Iwasaka, S. Ueno, H. Yokoi, Y. Kakudate, S. Fujiwara, and M. Kawamura, Jpn. J. Appl. Phys. **34**, L991 (1995).
[15] H. Sugawara, N. Hirota, T. Homma, M. Ohta, K. Kitazawa, H. Yokoi, Y. Kakudate, S. Fujiwara, M. Kawamura, S. Ueno, and M. Iwasaka, J. Appl. Phys. **79**, 4721 (1996).
[16] See Supplemental Material at http://link.aps.org/supplemental/10.1103/PhysRevE.90.030301 for video clips demonstrating the creation and the various manipulations of the BM, including its underwater ignition capabilities.
[17] G. Kletetschka, P. J. Wasilewski, and P. T. Taylor, Phys. Earth Planet. Inter. **119**, 259 (2000).
[18] G. Lumay, S. Dorbolo, and N. Vandewalle, Phys. Rev. E **80**, 041302 (2009).
[19] H. G. Bruil and J. J. Van Aartsen, Colloid Polym. Sci. **252**, 32 (1974).
[20] A. A. Kulkarni and J. B. Joshi, Eng. Chem. Res. **44**, 5873 (2005).
[21] L. Chen, S. V. Garimella, J. A. Reizes, and E. Leonardi, J. Fluid Mech. **387**, 61 (1999).
[22] R. Clift, J. R. Grace, and M. Weber, *Bubbles, Drops, and Particles* (Academic Press, New York, 1978).
[23] A. Walther and A. H. E. Müller, Chem. Rev. **113**, 5194 (2013).
[24] Y. Meir and E. Jerby, Combust. Flame **159**, 2474 (2012).
[25] Y. Meir and E. Jerby, in *Proceedings of 14th International Conference on Microwave and High Frequency Heating, Sep. 16–19, 2013, Nottingham, UK* (University of Nottingham Department of Health Care of the Elderly, UK, 2013), pp. 61–64.
[26] H. Kawamoto and K. Tsuji, Adv. Powder Technol. **22**, 602 (2011).
[27] This hypothesis was proposed by an anonymous reviewer, suggesting that the BM reflective sheen might be a characteristic of a trapped layer of air around the outside as common to superhydrophobic surfaces (e.g., the *plastron* layer in insects' physiology, which enables them breathing under water [28]).
[28] N. J. Shirtcliffe, G. McHale, M. I. Newton, C. C. Perry, and F. B. Pyatt, Appl. Phys. Lett. **89**, 104106 (2006).